

# Activation Energy of $^{69}\text{Ga}$ , $^{71}\text{Ga}$ , and $^{75}\text{As}$ Nuclei in $\text{GaAs:Mn}^{2+}$ Single Crystal

Tae Ho Yeom<sup>1</sup> and Ae Ran Lim<sup>2\*</sup>

<sup>1</sup>Department of Laser and Optical Information Engineering, Cheongju University, Cheongju 360-764, Korea

<sup>2</sup>Department of Science Education, Jeonju University, Jeonju 560-759, Korea

(Received 8 February 2014, Received in final form 17 April 2014, Accepted 20 April 2014)

The spin-lattice relaxation time,  $T_1$ , for  $^{69}\text{Ga}$ ,  $^{71}\text{Ga}$ , and  $^{75}\text{As}$  nuclei in  $\text{GaAs:Mn}^{2+}$  single crystals was measured as a function of temperature. The values of  $T_1$  for  $^{69}\text{Ga}$ ,  $^{71}\text{Ga}$ , and  $^{75}\text{As}$  nuclei were found to decrease with increasing temperature. The  $T_1$  values in  $\text{GaAs:Mn}^{2+}$  crystal are similar to those in pure GaAs crystal. The calculated activation energies for the  $^{69}\text{Ga}$ ,  $^{71}\text{Ga}$ , and  $^{75}\text{As}$  nuclei are 4.34, 4.07, and 3.99 kJ/mol. It turns out that the paramagnetic impurity effect of  $\text{Mn}^{2+}$  ion doped in GaAs single crystal was not strong on the spin-lattice relaxation time.

**Keywords :** paramagnetic ions, nuclear magnetic resonance (NMR), activation energy, relaxation time

## 1. Introduction

Gallium arsenide, GaAs, is an important semiconductor material for various electronic and photonic devices, such as high-performance integrated circuits, field-effect transistors, light-emitting diodes, electroluminescent, and photo-detectors [1-3]. Because of its high saturated-electron velocity and excellent electron mobility, GaAs-based devices can be operated at higher frequencies and power levels with less noise than their silicon-based counterparts can. GaAs is also frequently used for lasers as a saturated absorber, infrared output coupler, and frequency-converting unit [4-7]. Semi-insulating GaAs is a suitable material for fabrication of particle detectors used in high-energy and nuclear physics [8, 9]. In another interesting application, GaAs is adopted as a detector of thermal neutrons [10, 11]. Direct-gap GaAs semiconductors are also promising materials for solar cell applications because they have higher efficiency than silicon cells [12-14].

When making electronic devices, the GaAs substrates need to have excellent surface integrity because lattice or structural defects would dramatically affect the performance of the devices. In this regard, it is scientifically and technologically important to understand the formation mechanism of lattice defects, including impurities. To control their optical and electrical properties during growth,

it is crucial to understand the thermodynamics of atomic defects in GaAs.

Because of their many fascinating properties, which are not only fundamentally important but also of immense commercial importance, the optical properties of materials containing transition and rare-earth metal ions have attracted the attention of physicists, chemists, and materials scientists for a long time [15]. Transition metals are well recognized as occupying a special place in the study of impurity defects in semiconductors [16]. Rare-earth element doping of GaAs is also currently under investigation due to the interest in this material for technological applications. The impurity photovoltaic effect in GaAs solar cells is based on incorporating impurities with deep impurity levels [17]. GaAs, highly doped by  $\text{Mn}^{2+}$ , has the properties of a diluted magnetic semiconductor. It is the main candidate as the basic material for optoelectronic spintronic devices [18, 19].

Magnetic resonance studies are very important for investigating microscopic information such as the local site symmetry, substitutional sites of impurity ions, clusters, and the dynamics of the host nuclei in the crystal [20]. Electron spin resonance in donors in *n*-GaAs [21] and Mn centers in *p*-type GaAs crystals [22] has been studied. A beta-detected nuclear magnetic resonance (NMR) experiment has been carried out to investigate the magnetic properties of a semi-insulating GaAs crystal [23]. NMR spectroscopy of a GaAs epitaxial layer [24] and nuclear magnetic relaxation of host nuclei in GaAs [25] have also been studied.

©The Korean Magnetism Society. All rights reserved.

\*Corresponding author: Tel: +82-63-220-2514

Fax: +82-63-220-2053, e-mail: [aeranlim@hanmail.net](mailto:aeranlim@hanmail.net)

In general, the nuclear spin-lattice relaxation of nuclei is influenced by the paramagnetic impurities in a crystal. In this work, the spin-lattice relaxation times of  $^{69}\text{Ga}$ ,  $^{71}\text{Ga}$ , and  $^{75}\text{As}$  nuclei in a  $\text{GaAs:Mn}^{2+}$  single crystal is investigated with a Fourier transform NMR spectrometer. The effect of the paramagnetic  $\text{Mn}^{2+}$  impurity on the relaxation of the host nuclei is also discussed. The detailed information about the dynamics of GaAs crystals doped with paramagnetic impurity  $\text{Mn}^{2+}$  is obtained by measuring the spin-lattice relaxation time,  $T_1$ , of their constituent nuclei,  $^{69}\text{Ga}$ ,  $^{71}\text{Ga}$ , and  $^{75}\text{As}$ .

## 2. Experiment

The NMR spectrum of the  $^{69}\text{Ga}$ ,  $^{71}\text{Ga}$ , and  $^{75}\text{As}$  nuclei in a  $\text{GaAs:Mn}^{2+}$  single crystal were measured using a Bruker 400 MHz FT NMR spectrometer at the Korea Basic Science Institute. The static magnetic field was 9.4 T and the central radio frequency was set to  $\omega_0/2\pi = 96.061$ , 122.057, and 68.509 MHz for the  $^{69}\text{Ga}$ ,  $^{71}\text{Ga}$ , and  $^{75}\text{As}$  nuclei, respectively. The spin-lattice relaxation times were measured using the inversion-recovery pulse sequence,  $\pi-t-\pi/2$ . The nuclear magnetizations of the  $^{69}\text{Ga}$ ,  $^{71}\text{Ga}$ , and  $^{75}\text{As}$  nuclei at time  $t$  after the  $\pi$  pulse, a combination of one hundred  $\pi/2$  pulses applied at regular intervals, were determined following the  $\pi/2$  excitation pulse. The width of the  $\pi/2$  pulse was 1 and 5  $\mu\text{s}$  for the  $^{69}\text{Ga}$  and  $^{71}\text{Ga}$  nuclei, respectively, and 5  $\mu\text{s}$  for the  $^{75}\text{As}$  nucleus. The temperature-dependent NMR measurements were obtained over a temperature range of 180-420 K. The samples were maintained at constant temperatures by controlling the nitrogen gas flow and the heater current.

## 3. Results and Analysis

Here, we describe the inversion recovery laws for the quadrupole relaxation processes in the  $^{69}\text{Ga}$  ( $I = 3/2$ , natural abundance: 60.4%),  $^{71}\text{Ga}$  ( $I = 3/2$ , natural abundance: 39.6%), and  $^{75}\text{As}$  ( $I = 3/2$ , natural abundance: 100%) nuclear spin systems. The transition probabilities for  $\Delta m = \pm 1$  and  $\Delta m = \pm 2$  are denoted by  $W_1$  and  $W_2$ , respectively. The rate equations can then be expressed as [26]:

$$\begin{aligned} dn_{-3/2}/dt &= -(W_1 + W_2)n_{-3/2} + W_1 n_{-1/2} + W_2 n_{1/2} \\ dn_{-1/2}/dt &= W_1 n_{-3/2} - (W_1 + W_2)n_{-1/2} + W_2 n_{3/2} \\ dn_{1/2}/dt &= W_2 n_{-3/2} - (W_1 + W_2)n_{1/2} + W_1 n_{3/2} \\ dn_{3/2}/dt &= W_2 n_{-1/2} + W_1 n_{1/2} - (W_1 + W_2)n_{3/2} \end{aligned} \quad (1)$$

where  $n_{-3/2}$ ,  $n_{-1/2}$ ,  $n_{1/2}$ , and  $n_{3/2}$  are the population differences, with respect to the equilibrium population, at time  $t$  for each energy level. The eigenvalues of these equations are  $W_1$ ,  $W_2$ , and  $W_1 + W_2$ .

The inversion recovery traces for the resonance lines of  $^{69}\text{Ga}$ ,  $^{71}\text{Ga}$ , and  $^{75}\text{As}$  with dominant quadrupole relaxation can be represented as a combination of two exponential functions [26, 27]:

$$[M(\infty) - M(t)]/2M(\infty) = 0.5 [\exp(-2W_1 t) + \exp(-2W_2 t)] \quad (2)$$

where  $M(t)$  is the nuclear magnetization corresponding to the central transition at time  $t$  after saturation. The spin-lattice relaxation rate is given by [26]

$$1/T_1 = 2W_1 \text{ in case of } W_1 = W_2 \quad (3)$$

$$1/T_1 = 0.4 (W_1 + 4W_2) \text{ in case of } W_1 \neq W_2. \quad (4)$$

It is well known that a relaxation time  $T_1$  can be defined only if the time dependence of the magnetization can be described by a single-exponential relaxation function. Of course, one might introduce a useful combination of the transition probabilities  $W_1$  and  $W_2$  according to Eq. (2) and then explain that the introduction of this constant is reasonable because it leads to the correct relaxation time  $T_1 = 1/(2W_1)$  in the case of  $W_1 = W_2$ . Then, a single exponential relaxation function can be derived from Eq. (3).

The  $^{69}\text{Ga}$  and  $^{71}\text{Ga}$  NMR spectra in a  $\text{GaAs:Mn}^{2+}$  single

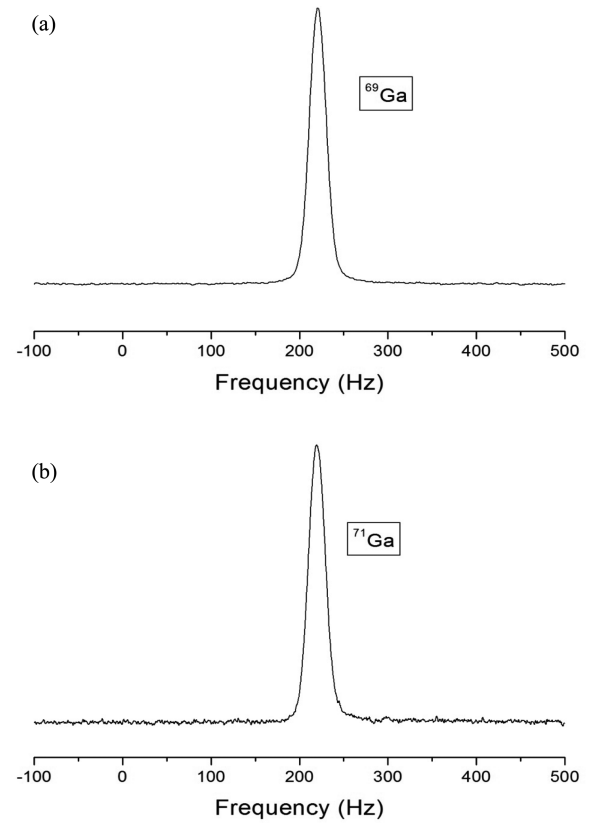


**Fig. 1.** (a)  $^{69}\text{Ga}$  and (b)  $^{71}\text{Ga}$  NMR spectra in a  $\text{GaAs:Mn}^{2+}$  single crystal at room temperature.

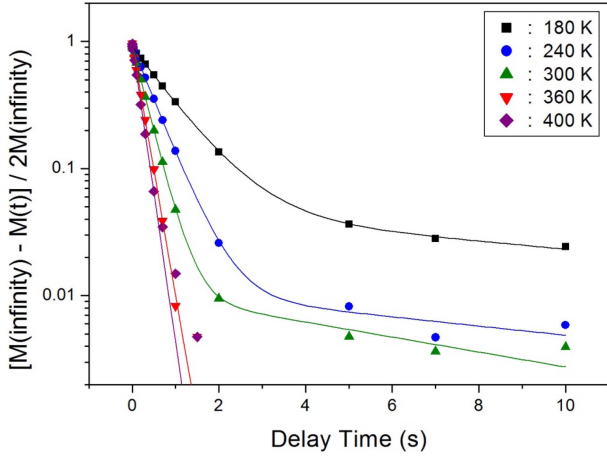


**Fig. 2.** (Color online) Magnetization recovery traces of  $^{71}\text{Ga}$  nuclei as a function of delay time at several temperatures. The solid lines are fitted with Eq. (2).

crystal at room temperature are shown in Fig. 1(a) and (b), respectively. These spectra were obtained by a Fourier transform of the Ga ( $I = 3/2$ ) NMR spectrum. Only one signal was detected for each nucleus, no matter where the magnetic field was applied, which implies that the nuclei are arranged in a cubic symmetry and that the resulting electric field gradient around them vanishes. The line-widths for  $^{69}\text{Ga}$  and  $^{71}\text{Ga}$  at 300 K were the same, at about 23 Hz, and nearly constant with temperature.

The  $^{69}\text{Ga}$  and  $^{71}\text{Ga}$  spin–lattice relaxation times  $T_1$  were measured using the inversion recovery method for the resonance line of the Ga nuclei. The magnetization recovery traces for the  $^{71}\text{Ga}$  nucleus were measured at several temperatures, as shown in Fig. 2. The recovery traces for the resonance line of Ga, with dominant quadrupole relaxation, can be expressed as a combination of two exponential functions, as in Eq. (2). Here, the slope of the plot of  $\log[(M(\infty) - M(t))/2M(\infty)]$  versus time  $t$  below room temperature was not linear, because the traces were composed of a combination of two exponential functions. In general,  $W_1$  is less than  $W_2$  at all temperatures. In case of low temperature (180 K, 240 K, 300 K), the  $T_1$  can be obtained with  $5/[2(W_1 + 4W_2)]$  when  $W_1 \neq W_2$ . However,  $W_1$  and  $W_2$  are the same in high temperatures of 360 K and 400 K. Thus, we can define relaxation times  $T_1$  according to  $T_1 = 1/(2W_1)$ , and the recovery trace can thus be represented by a single exponential function as shown in Fig. 2. The magnetization recovery traces for the  $^{69}\text{Ga}$  nucleus measured at several temperatures were similar with those for the  $^{71}\text{Ga}$  nuclei in Fig. 2.

The temperature dependences of the spin-lattice relaxation time  $T_1$  for the  $^{69}\text{Ga}$  and  $^{71}\text{Ga}$  nuclei in a  $\text{GaAs:Mn}^{2+}$  single crystal are shown in Fig. 3. The relaxation times of

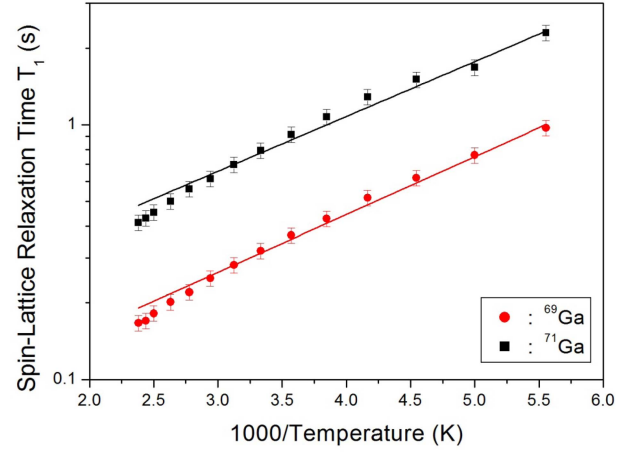


**Fig. 3.** (Color online) Temperature dependences of the spin–lattice relaxation time  $T_1$  for  $^{69}\text{Ga}$  and  $^{71}\text{Ga}$  in a  $\text{GaAs:Mn}^{2+}$  single crystal. The slope of the solid line represents the activation energy.

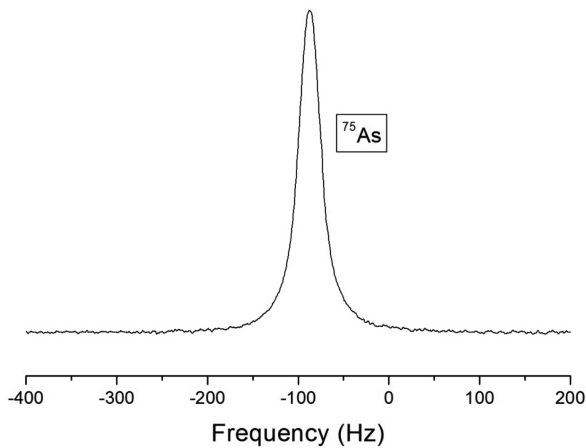
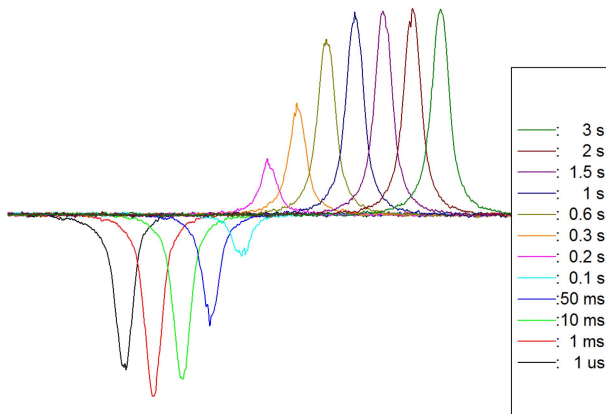
$^{71}\text{Ga}$  nuclei at 200 K, 300 K, and 400 K are 1678 ms, 792 ms, and 453 ms, respectively. The spin–lattice relaxation times  $T_1$  for  $^{71}\text{Ga}$  are longer than those for  $^{69}\text{Ga}$  in the same temperatures. This difference is due to the difference in magnitude of the electric quadrupole moments of  $^{69}\text{Ga}$  and  $^{71}\text{Ga}$  ( $Q_{\text{Ga}(69)} = 17.1 \times 10^{-30} \text{ m}^2$  and  $Q_{\text{Ga}(71)} = 10.7 \times 10^{-30} \text{ m}^2$ ); the spin–lattice relaxation rate was proportional to the square of the quadrupole coupling constant [26]. The relaxation times for both  $^{69}\text{Ga}$  and  $^{71}\text{Ga}$  nuclei decrease with increasing temperature. There is no any abrupt change of relaxation times in the temperature range of 180–420 K, which indicates that no phase transitions occur within the experimental temperature range.

The activation energies of  $^{69}\text{Ga}$  and  $^{71}\text{Ga}$  nuclei in  $\text{GaAs:Mn}^{2+}$  crystals were determined using the equation  $T_1 = A_o \exp(E_a/k_B T)$ , where  $E_a$  and  $A_o$  are the activation energy and the pre-exponential factor, respectively, while  $k_B$  and  $T$  are the Boltzmann constant and the temperature, respectively. A plot of the natural logarithm of  $T_1$  as a function of inverse temperature is hence linear, with a slope that is directly related to the activation energy. The activation energies for the  $^{69}\text{Ga}$  and  $^{71}\text{Ga}$  nuclei are  $4.34 \pm 0.11$  and  $4.07 \pm 0.14$  kJ/mol for  $\text{GaAs:Mn}^{2+}$  crystals, respectively, while the factor  $A_o$  is 0.054 and 0.148, respectively, as shown in Table 1.

Typical NMR spectra of  $^{75}\text{As}$  in the  $\text{GaAs:Mn}^{2+}$  crystal along the  $c$ -axis at room temperature are shown in Fig. 4. Instead of the three resonance lines obtained for  $^{75}\text{As}$  nuclei in GaAs crystals, only one resonance line for  $^{75}\text{As}$  was obtained across the temperature range investigated. This indicates that  $^{75}\text{As}$  nuclei in  $\text{GaAs:Mn}^{2+}$  reside in cubic site. In a cubic crystal, the electric quadrupole

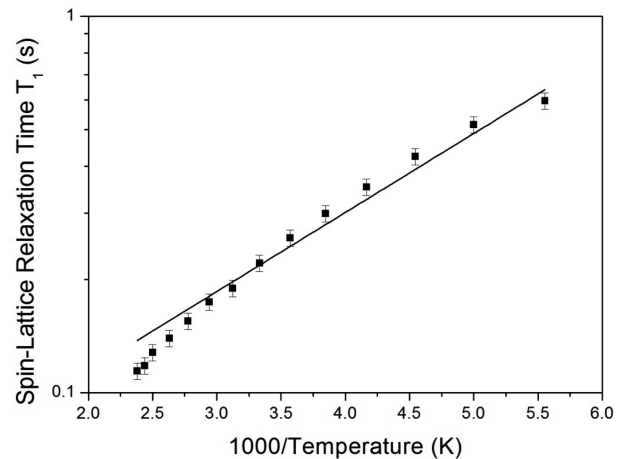
**Table 1.** The pre-exponential factor  $A_0$  and activation energy  $E_a$  for  $^{65}\text{Ga}$ ,  $^{71}\text{Ga}$ , and  $^{75}\text{As}$  in GaAs:  $\text{Mn}^{2+}$  single crystals.

| Nucleus          | $A_0$ | $E_a$ (kJ/mol)  |
|------------------|-------|-----------------|
| $^{65}\text{Ga}$ | 0.054 | $4.34 \pm 0.11$ |
| $^{71}\text{Ga}$ | 0.148 | $4.07 \pm 0.14$ |
| $^{75}\text{As}$ | 0.043 | $3.99 \pm 0.16$ |

**Fig. 4.**  $^{75}\text{As}$  NMR spectrum in a GaAs:  $\text{Mn}^{2+}$  single crystal at room temperature.**Fig. 5.** (Color online) Inversion recovery traces of  $^{75}\text{As}$  nuclei as a function of delay time at room temperature.

moments of the  $^{75}\text{As}$  nucleus cause no perturbation of the four nuclear Zeeman levels, so all transitions contribute to a single resonance line. The line-width for  $^{75}\text{As}$  at room temperature is about 28 Hz, which is similar to those of the  $^{69}\text{Ga}$  and  $^{71}\text{Ga}$  nuclei in Fig. 1.

Figure 5 shows the inversion recovery traces for the resonance line of  $^{75}\text{As}$  nuclei in GaAs:  $\text{Mn}^{2+}$  crystals at room temperature for delay times ranging from 1  $\mu\text{s}$  to 3 s. The magnetization recovery trace for  $^{75}\text{As}$  was deter-

**Fig. 6.** Temperature dependence of the spin-lattice relaxation time  $T_1$  for  $^{75}\text{As}$  in a GaAs:  $\text{Mn}^{2+}$  single crystal. The slope of the solid line represents the activation energy.

mined from the time evolution of the resonance spectrum with respect to the delay time and then obtained with the inversion recovery method. The inversion recovery traces vary with delay time. The recovery traces for the resonance line of  $^{75}\text{As}$  with dominant quadrupole relaxations in GaAs can be represented by a combination of two exponential functions, as shown in Eq. (2). These recovery traces varied depending on the temperature, and their slopes increased with increasing temperature. The trends of temperature dependences for  $W_1$  and  $W_2$  of  $^{75}\text{As}$  nuclei were similar each other, with  $W_1$  being consistently smaller than  $W_2$ . The relaxation times of  $^{75}\text{As}$  nuclei in GaAs:  $\text{Mn}^{2+}$  were obtained from Eq. (4) using the values of  $W_1$  and  $W_2$ .

The  $^{75}\text{As}$  spin-lattice relaxation time  $T_1$  was obtained in the temperature range of 180–420 K as shown in Fig. 6. The relaxation time  $T_1$  for  $^{75}\text{As}$  is much smaller than that for both  $^{69}\text{Ga}$  and  $^{71}\text{Ga}$  nuclei in Fig. 3. The smaller  $T_1$  of  $^{75}\text{As}$  may originate from the larger quadrupole moment of As nucleus ( $Q_{\text{As}(75)} = 31.4 \times 10^{-30} \text{ m}^2$ ) compare with Ga nuclei. The  $\text{Mn}^{2+}$  impurity effect on the smaller  $T_1$  of  $^{75}\text{As}$  seems to be negligible. The spin-lattice relaxation time  $T_1$  for  $^{75}\text{As}$  in GaAs:  $\text{Mn}^{2+}$  single crystal decreases with increasing temperature, as shown in Fig. 6. The relaxation time of the  $^{75}\text{As}$  nuclei undergoes no abrupt changes within the experimental temperature range, which indicates that no phase transitions occur within the temperature range. The activation energy of  $^{75}\text{As}$  in GaAs:  $\text{Mn}^{2+}$  single crystals was then determined. The activation energy and  $A_0$  for  $^{75}\text{As}$  are  $3.99 \pm 0.16$  kJ/mol and 0.043, respectively, as shown in Table 1.

In studies of experimental relaxation rate for the  $^{69}\text{Ga}$ ,

$^{71}\text{Ga}$ , and  $^{75}\text{As}$  nuclei, it is important to know whether the relaxation rate is located on the slow side of the minimum or on the fast side of the minimum as a function of the inverse temperature. The general behavior of the spin-lattice relaxation rate for random motions of the Arrhenius type with a correlation time  $\tau_c$  can be described in terms of regions of fast and slow motions as follows [28]:

$$\begin{aligned} \omega_o\tau_c \ll 1, T_1^{-1} &\sim \exp[E_a/RT] \text{ (fast motion)} \\ \omega_o\tau_c \gg 1, T_1^{-1} &\sim \omega_o^{-2}\exp[-E_a/RT] \text{ (slow motion)} \end{aligned} \quad (5)$$

where  $\omega_o$  is the Larmor frequency and  $E_a$  is the activation energy. For the  $^{69}\text{Ga}$ ,  $^{71}\text{Ga}$ , and  $^{75}\text{As}$  nuclei in  $\text{GaAs:Mn}^{2+}$  crystal, the spin-lattice relaxation time is in the slow motion region in the experimental temperature range.

#### 4. Conclusion

The relaxation processes in  $\text{GaAs:Mn}^{2+}$  crystals were investigated by determining the spin-lattice relaxation times of the  $^{69}\text{Ga}$ ,  $^{71}\text{Ga}$ , and  $^{75}\text{As}$  nuclei. The spin-lattice relaxation time  $T_1$  for  $^{69}\text{Ga}$  was shorter than that for  $^{71}\text{Ga}$  at the same temperature. This difference is due to the difference in magnitude of the electric quadrupole moments of the two isotopes  $^{69}\text{Ga}$  and  $^{71}\text{Ga}$ . In addition, the relaxation time for  $^{75}\text{As}$  is much smaller than for both  $^{69}\text{Ga}$  and  $^{71}\text{Ga}$  nuclei. The relaxation times  $T_1$  for  $^{69}\text{Ga}$ ,  $^{71}\text{Ga}$ , and  $^{75}\text{As}$  nuclei in  $\text{GaAs:Mn}^{2+}$  crystal are similar to those obtained in pure  $\text{GaAs}$  single crystal [25]. The paramagnetic impurity effect on the spin-lattice relaxation process for host nuclei in  $\text{GaAs:Mn}^{2+}$  crystal was not strong within the experimental temperature range. Activation energy  $E_a$  of  $^{69}\text{Ga}$ ,  $^{71}\text{Ga}$ , and  $^{75}\text{As}$  nuclei in  $\text{GaAs:Mn}^{2+}$  crystal were determined in the temperature dependence of relaxation rate. The activation energy for each host nuclei in  $\text{GaAs:Mn}^{2+}$  has nearly the same values as shown in Table 1. The relaxation time of the  $^{69}\text{Ga}$ ,  $^{71}\text{Ga}$ , and  $^{75}\text{As}$  nuclei undergoes no abrupt changes in the temperature range 180-420 K, which indicates that no phase transitions occur within the experimental temperature range.

#### References

- [1] S. M. Sze, *Semiconductor Devices: An Introduction*, McGraw-Hill, New York, 1994.
- [2] X. A. Zhu and C. T. Tsai, *Computational Materials Science* **29**, 334 (2004).
- [3] Y. Q. Wua and H. Huang, J. Zou, *Materials Letters* **80**, 187 (2012).
- [4] T. T. Kajara and A. L. Gaeta, *Opt. Lett.* **21**, 1244 (1996).
- [5] S. Y. Tochitsky, J. E. Ralph, C. Sung, and C. Joshi, *J. Appl. Phys.* **98**, 026101 (2005).
- [6] D. Li, S. Zhao, G. Li, and K. Yang, *Optik* **121**, 478 (2010).
- [7] H. Qi, Q. Wang, X. Zhang, Z. Liu, S. Zhang, J. Chang, W. Xia, and G. Jin, *Optics and Lasers in Engineering* **49**, 285 (2011).
- [8] C. del Papa, P. G. Pelfer, and K. Smith, Erice (Eds.), *Proceedings of the 20th Workshop on GaAs Detectors and Electronics for High Energy Physics*, World Scientific, Singapore (1992).
- [9] *Experiments at CERN in 1993*, Geneve 1993, ISSN 0259-093X.
- [10] D. S. Mc Gregor, J. T. Lindsay, C. C. Brannon, and R. W. Owses, *IEEE Trans. Nucl. Sci.* **43**, 1357 (1996).
- [11] D. S. Mc Gregor, J. T. Lindsay, C. C. Brennon, and R. W. Olsen, *Nucl. Instr. and Meth. A* **380**, 271 (1996).
- [12] J. J. Lion, and W. W. Wong, *Solar Energy Mater. Solar Cells* **28**, 9 (1992).
- [13] N. J. Ekins-Daukes, K. W. J. Barnham, J. P. Connolly, J. S. Roberts, and J. C. Clark, G. Hill, M. Mazzer, *Appl. Phys. Lett.* **75**, 4195 (1999).
- [14] M. A. Green, K. Emery, D. L. King, S. Igari, and W. Warta, *Progr. Photovoltaics: Res. Appl.* **14**, 455 (2006).
- [15] M. G. Brik and A. M. Srivastava, *Optical Materials*, **35**, 1776 (2013).
- [16] A. Majid, M. Z. Iqbal, A. Dadgar, and D. Bimberg, *Physica B* **340**, 362 (2003).
- [17] S. Khelifi, M. Burgelman, J. Verschraegen, and A. Belghachi, *Solar Energy Materials & Solar Cells* **92**, 1559 (2008).
- [18] D. Burger, S. Zhou, J. Grenzer, H. Reuther, W. Anwand, V. Gottschalch, M. Helm, and H. Schmidt, *Nucl. Instr. and Meth. in Physics Research B* **267**, 1626 (2009).
- [19] Yu. A. Danilov, V. P. Lesnikov, Yu. N. Nozdrin, V. V. Podolskii, M. V. Sapozhnikov, O. V. Vikhrova, and B. N. Zvonkov, *J. Magn. And Magn. Materials* **300**, e28 (2006).
- [20] S. H. Lee, T. H. Yeom, and S. Kim, *J. Magn.* **17**, 251 (2012).
- [21] J. S. Colton, T. A. Kennedy, A. S. Bracker, and J. B. Miller, D. Gammon, *Solid State Commun.* **132**, 613 (2004).
- [22] Y. J. Park, E. K. Kim, S. K. Min, I. W. Park, and T. H. Yeom, *J. Korean Phys. Soc.* **30**, S113 (1997).
- [23] Q. Song, K. H. Chow, M. D. Hossain, R. F. Kiefl, G. D. Morris, C. D. P. Levy, H. Saadaoui, M. Smadella, D. Wang, B. Kardasz, B. Heinrich, and W. A. MacFarlane, *Physics Procedia* **30**, 227 (2012).
- [24] D. A. Alexson and D. D. Smith, *J. Magn. Reson.* **235**, 66 (2013).
- [25] T. H. Yeom, I. G. Kim, S. H. Choh, K. S. Hong, Y. J. Park, and S. K. Min, *Solid State Commun.* **111**, 229 (1999).
- [26] A. Abragam, *The Principles of Nuclear Magnetism*, Chap. IX, Oxford University Press, Oxford (1961).
- [27] J. J. van der Klink, D. Rytz, F. Borsa, and U. T. Hochli, *Phys. Rev.* **B27**, 89 (1983).
- [28] A. R. Lim and S. Y. Jeong, *J. Phys.: Condens. Matter* **16**, 4403 (2004).